# Seminar: Charged exciton complexes (trions) in low dimensional structures

Dmitri Andronikov

June 17, 2005

**Abstract**

Photoluminescence (PL) and reflectivity spectra from modulation-doped CdTe/CdMgTe quantum well structures containing two dimensional electron gas have been studied in magnetic field as high as 45T. A recombination line of a dark triplet trion state was observed in the PL spectra. PL intensity was calculated in the magnetic field taking into account singlet and triplet trion states. It was shown that the dark triplet becomes visible in the PL spectra since it becomes the only recombination channel when the formation of the singlet trion state is suppressed by magnetic field.

# Contents

# 1 Introduction

## 1.1 What are trions

Charged excitons or trions represent bound states of three particles. They are formed of two electrons and a hole in the case of negatively charged excitons (similar to ionized hydrogen atom $H^-$), and two holes and one electron in the case of positively charged excitons (similar to ionized hydrogen atom $H_2^+$). [KCM+93]

## 1.2 Short history of trions

Short history of trions:
1) In 1958 Lampert first predicted the existence of bound three particle states similar to hydrogen atoms in semiconductors.
2) In 1977-78 charged excitons were discovered in bulk Ge, Si and CuCl.
3) In 1993 the first report on $X^-$ in CdTe/CdZnTe was published.
4) In 1995 the observation of $X^+$ trion in GaAs QW was reported.
Since then study of trions became very intensively developing field of semiconductor science.

## 1.3 Singlet and triplet trion states

Similar to a helium atom or a negatively charged hydrogen ion $H^-$ the negatively charged exciton complex – $X^-$ trion has two sets of states – triplet and singlet. [BS57]

The solution of the Shroedinger equation for $H^-$ or $X^-$ is the following wave function: $\varphi(1,2) = U(1,2)\chi(1,2)$, where $U$ is the spatial and $\chi$ is the spin part of the wave function. [BS57] Symmetrized and normalized spatial wave function of zero approximation can be chosen as:

$$U^0_{nlm} = \frac{1}{\sqrt{2}} \left[ u_1 \left( \vec{r}_1 \right) \, u_{nlm} \left( \vec{r}_2 \right) \pm u_1 \left( \vec{r}_2 \right) \, u_{nlm} \left( \vec{r}_1 \right) \right]. \tag{1}$$

Here $u_1$ corresponds to electron in the ground $1S$ state (we assume that one of the electrons is in the ground state); $n$, $l$ and $m$ are the main, azimuthal, and magnetic quantum numbers respectively. Plus stands for the singlet state, minus for the triplet states.

The singlet state corresponds to the full spin of two electrons $S_e = 0$. The spin part of the wave function is antisymmetrical to permutation of electrons and can be:

$$\chi_{singl} = (1/\sqrt{2}) \times [(+1/2, -1/2) - (-1/2, +1/2)]. \tag{2}$$

Here $\pm 1/2$ is the projection of the electron spin on $z$ axis.

The spatial part of the wave function of such state is, vice versa, symmetrical to the permutation of electrons (plus in Eq.(1)). In this case both electrons can be in the $1S$ state, each with its own Bohr radius.

Triplet states correspond to the full spin of two electrons $S_e = 1$ with three possible projections on $z$ axis $S_z = \pm 1{,}0$. Three spin wave functions are:

$$\chi^{+1}_{trip} = (+1/2, +1/2)\,,$$

$$\chi^{0}_{trip} = (1/\sqrt{2}) \times [(+1/2, -1/2) + (-1/2, +1/2)], \tag{3}$$

$$\chi^{-1}_{trip} = (-1/2, -1/2)\,.$$

The spatial part of the wave function of the triplet state is antisymmetrical to permutation of electrons (minus in Eq.(1)). It is obvious that if both electrons are in the ground state ($n = 1, l = m = 0$ in Eq.1) the wave function is zero.

The wave function of the triplet state will not be equal to zero only if the electrons are occupied different orbitals ($1S$ and $2S$ i.e. $n = 2, \quad l = m = 0$ in Equation 1) or if the full orbital momentum of the electrons is not zero (one electron is on $1S$ orbital and a second on $2P$ orbital i.e. $l \neq 0$ in Eq.1).

From this follows, that the state which is the lowest in energy should be the singlet state when both electrons are in the ground state.

Thus the energy level scheme of the $X^-$ trion consists of two systems of sublevels. One system contains three triplet levels with the projection of the full spin of two electrons on $z$ axis $S_z = \pm 1, 0$. The other contains one singlet level with $S_z = 0$. The singlet level is energetically lower than the triplet levels and is the ground state of the two-electron system. The scheme of the trion spin states and optical transitions is shown in Fig. **??**.

### 1.4 Binding energies of excitons and trions in 2D and 3D case

Now let's see how the binding energies of excitons and trions change when we go from bulk materials to quasi-2D materials such as QWs. The binding energy of the hydrogen atom ground state is 13.6 eV. For bulk exciton this value is sufficiently lower and is of the order of 10-th of meV. Trion bulk energies are even less - lower than 1 meV. Thus in optics the bulk trion is almost not observable. When we go from 3D to 2D the exciton binding energy increases 4 times compared to that of bulk material. Since QW is not a perfectly 2D object the energy increase is lower. The trion binding energy also increases reaching 5 meV in 100Å ZnSe QW. This makes QWs very good structures to study trions.

## 2 Experiment

We studied CdTe/$Cd_{0.7}Mg_{0.3}$Te heterostrucutres with a single 100Å quantum well (QW)grown by MBE on (100) GaAs substrate. To minimize the number of dislocations due to the difference in lattice constants of the QW and barrier materials the quantum well was grown after a CdTe buffer layer (about 400 nm thick).

An iodine n-type $\delta$-layer is located on a distance of 100Å from the well. At low temperatures electrons from the $\delta$-layer are collected in the quantum well forming a quasi-2D electron gas (2DEG). We studied a set of such heterostructures grown during one epitaxy using wage doping technique. [WKK$^+$97] All the QWs have the same parameters and are different only in the doping level in the $\delta$-layer (and therefore the 2DEG density). The electron concentrations in the QWs varied within the range from $10^{10}$ cm$^{-2}$ to $10^{12}$ cm$^{-2}$. The samples were not photosensitive, i.e. the electron concentration did not depend on the power of the additional illumination.

Polarized photoluminescence and reflectivity from these samples were measured in magnetic fields applied in the Faraday configuration. A capacitor-driven 50T mid-pulse magnet (400 ms pulse duration) was used to yield high magnetic fields. A complete set of field-dependent PL spectra excited by a semiconductor diode laser with $\lambda = 532$ nm at 1.6K, 4.2K and 15K temperature was collected during each magnet pulse. Optical fibers were used for optical illumination of the sample, and the emitted light was detected in both circular polarizations $\sigma^+$ and $\sigma^-$ allowing identification of the spin components of excitons and trions. A similar setup was used for reflectivity measurements with a halogen lamp as a light source.

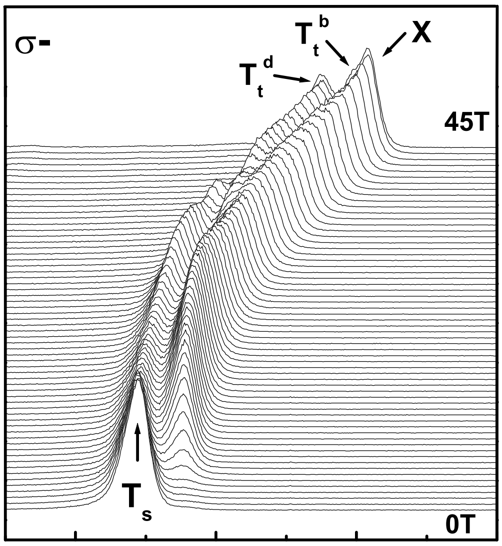


Figure 1: Set of photoluminescence spectra taken in the magnetic fields from 0 to 45T from the sample with $n_e = 3 * 10^{10}$ cm$^{-2}$ in $\sigma^-$ circular polarization. $X$ - the exciton line, $T_s$ – the singlet trion line, $T_t^d$ – the dark triplet trion line, $T_t^b$ – the bright triplet trion line.

# 3 Results and Discussion

## 3.1 Photoluminescence

A set of photoluminescence spectra registered from the sample with electron concentration $n_e$ = 3*10$^{10}$ cm$^{-2}$ in the range of magnetic fields from 0 to 45 T in left circular polarization $\sigma^-$ is shown in Fig. 1. We do not show the PL spectra in $\sigma^+$ polarization because the signals are too weak.

In low magnetic fields a bright PL line $T_s$ is observed in $\sigma^-$ polarization at the energy of 1.614 eV. This line corresponds to the singlet state of the trion. In the low magnetic field the neutral exciton line $X$ is visible only as a small shoulder shifted by 3 meV from the singlet trion line towards higher energy. By increase of the magnetic field the intensity of the luminescence of the singlet trion line drops while the intensity of the exciton line rises. One more bright line $T_t^d$ appears in the spectra in the magnetic fields higher 24 Tesla in the energy range between $T_s$ and $X$ lines. As magnetic field grows its intensity increases as well.

Fig. 2 shows the magnetic field dependence of the energy positions of all PL lines in both circular polarizations. The lines of the neutral exciton $X$ and singlet trion $T_s$ experience nearly equal diamagnetic shift towards higher energies. The Zeeman splitting of these lines is also identical. The $T_t^d$ line is observed only in $\sigma^-$ polarization. It shifts from the exciton line towards lower energies. In the maximal field of 45T it splitting from the exciton line amounts to about 3 meV.

As was mentioned before, the energetically lowest triplet state has the projection of the orbital momentum in the direction of the magnetic field $L_z = -1$, which is optically forbidden. From the energy position of the $T_t^d$ line and its polarization we associate this line with the recombination of the optically forbidden triplet trion with $z$ projection of the total spin $S_z^tr = -1/2$ and $z$ projection of the orbital angular momentum $L_z = -1$.

In the fields higher than 35 T another PL line was observed in $\sigma^-$ circular polarization shifted by $\propto$1 meV from the exciton line towards lower energy. It is marked in Fig. 1 and Fig. 2 as $T_t^b$.

The triplet trion also has optically active states [RPV01, WQH00] that are energetically

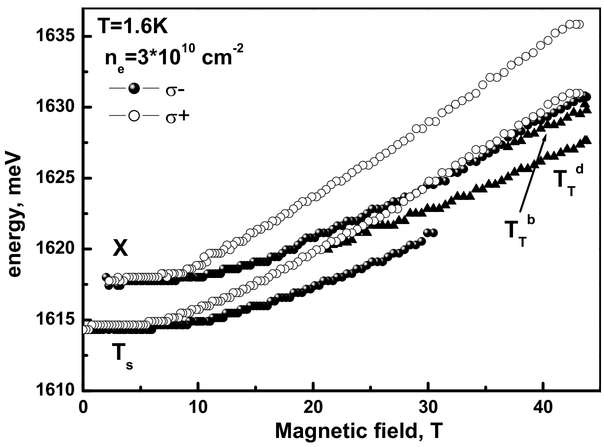


Figure 2: Magnetic field dependence of the energy positions for all PL lines. Open circles stand for $\sigma^+$ polarization, closed circles stand for $\sigma^-$ polarization. Triangles indicate triplet trion states observed only in $\sigma^-$ polarization. $X$ indicates the states of optically active exciton in the corresponding polarization $\sigma^+$ or $\sigma^-$. $T_s$ - indicates the states of the singlet trion in corresponding polarization. $T_t^d$ is optically dark due to the orbital momentum triplet trion state, and $T_t^b$ is the bright triplet trion state with $L_z = 0$.

higher than the dark state. In this case one of the electrons is on the first and the other is on the second Landau level ($n = 2, l = m = 0$ in Eq.1.) The state has the orbital momentum $L$ =0 and $z$ projection of the total spin $S_z^t r = -1/2$, therefore corresponded transitions are optically allowed. We ascribe the PL line $T_t^b$ to one of the optically active triplet trion states.

## 3.2 Reflectivity

Optically inactive states cannot be observed in reflectivity, which means that the $T_t^d$ line observed in the PL should be invisible in reflectivity. At the same time the bright trion states with the orbital momentum $L = 0$ should show up.

In Fig. 3 reflectivity spectra taken from the sample with electron concentration $n_e = 3 * 10^{10}$ cm $^{-2}$ are compared with the corresponding luminescence spectra in 6, 27 and 45 Tesla in $\sigma^+$ and $\sigma^-$ polarizations. The energy positions of the $T_s$ and $X$ reflection lines coincide with the positions of these lines in the PL spectra. The Stocks shift does not exceed 0.3 meV. The singlet trion line is already fully polarized in the magnetic field as low as 6T and is observed in $\sigma^+$ polarization only, which signifies full spin polarization of the 2DEG in the magnetic field [AKY$^+$02] for this sample. We have found no reflectivity line, which could correspond to the $T_t^d$ line in the PL spectrum. This confirms the assumption that the $T_t^d$ line in PL corresponds to the recombination of the dark triplet trion.

In high magnetic fields a shoulder marked as $T_t^b$ in Fig. 3 appears in the reflectivity spectra in the vicinity of the lowest Zeeman component of the exciton line. Its energy position at 45 T ($\hbar\omega = 1629.5meV$) coincides with that of the $T_t^b$ line in the PL spectra. This small shoulder in the reflectivity spectra, as well as the line $T_t^b$ in the PL spectra, corresponds to the optically active triplet trion state with orbital momentum $L = 0$.

We used the fit by Gaussian functions to separate the contributions from exciton, singlet and triplet trion into the PL spectrum as shown in Fig. 3

Fig. 4 shows the dependences of the intensities all the luminescence lines in the sample with electron concentration $n_e = 3 * 10^{10}$ cm$^{-2}$. In low magnetic fields the intensity of the PL line of the singlet trion significantly exceeds that of the exciton due to the fast trion formation rate. As the magnetic field grows the intensity of the singlet trion luminescence line falls in

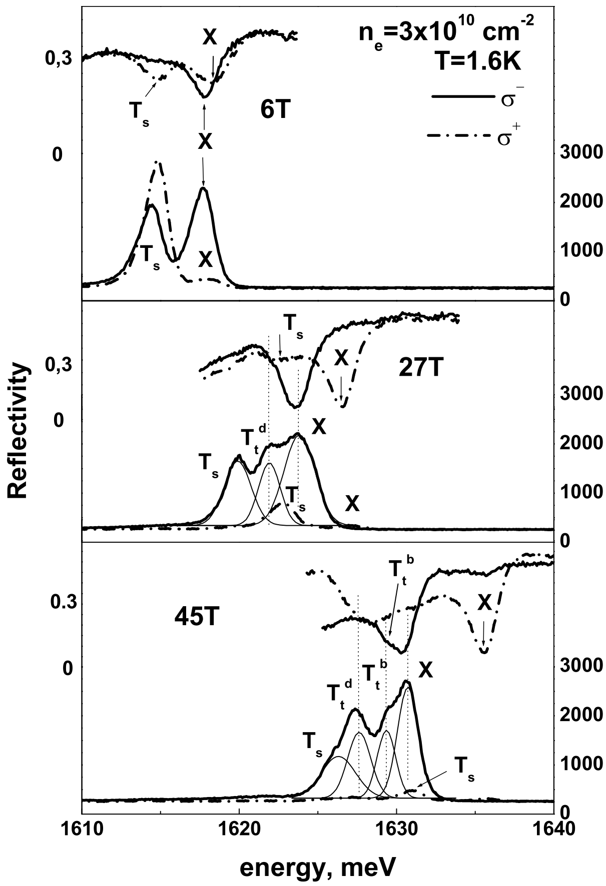


Figure 3: Reflectivity and photoluminescence spectra taken from the sample with electron concentration $n_e = 3 * 10^{10} cm^{-2}$ in the magnetic fields 6T, 27T and 45T. Heavy solid lines are used for $\sigma^-$ polarization, dashed-dotted lines - for $\sigma^+$ polarization. Light solid lines are the result of the deconvolution of the PL spectra by Gaussian curves fit. Dotted straight lines are comparison of PL and reflectivity spectral features.

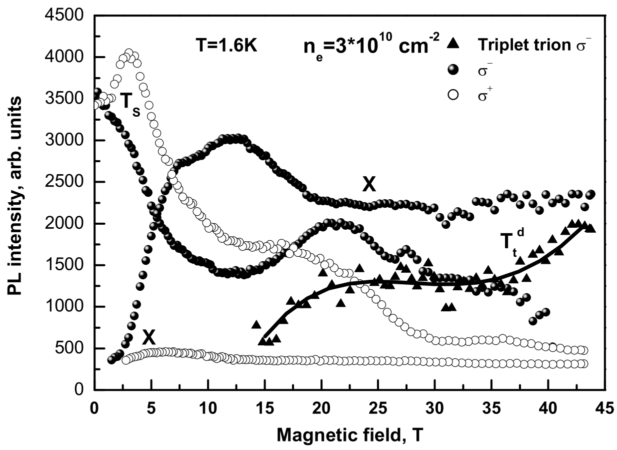


Figure 4: The magnetic field dependencies of the intensities of all PL lines. The dependence of the triplet trion line intensity was built by the Gauss fit of the exciton and triplet trion line. The designations are similar to those in Fig. 1. The intensity of the bright triplet line (not shown in the figure) is nearly equal to the intensity of the exciton line in the range of magnetic fields from 35T to 45T in which it is observable.

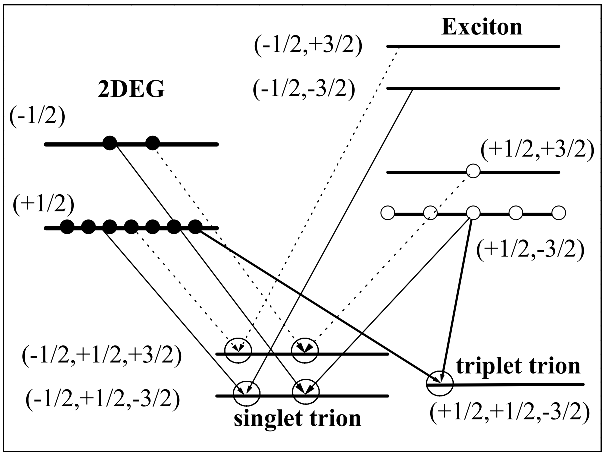


Figure 5: The scheme of the singlet and triplet trion formation mechanism.

both circular polarizations while the exciton line intensifies in the $\sigma^-$ polarization and remains weak in the $\sigma^+$ polarization.

The triplet trion photoluminescence line clearly appears in the spectra in magnetic fields of about 20 T. Its intensity weakly depends on the the magnetic field in the range between 25 T and 40 T.

In the magnetic field weaker than 20 T the triplet trion and exciton lines are so close to each other in energy that they cannot be easily distinguished visually. In order to separate their contours we used the Gaussian function fit. The broadened exciton PL line was fitted by two Gaussians with half widths of about 0.9 meV.

This way allowed us to plot the dependence of the intensity of the triplet trion PL line on the magnetic fields to the fields as low as 15 T. At lower magnetic fields the accuracy of the contour splitting noticeably falls. However one can claim that the triplet trion line is observable down to the fields of 5-7 T. Therefore, it means that in such low magnetic fields the triplet trion state remains bound and its PL line merges with these of exciton.

## 3.3 Singlet and triplet trion states formation mechanism

Let us examine in detail the mechanism of the singlet trion state formation (Fig. 5). There are two channels for the population of the upper Zeeman sublevel.

The upper Zeeman sublevel of the singlet trion becomes populated when the electrons from the lower sublevel ($S_z$=+1/2) and the excitons from the upper optically active sublevel (-1/2, +3/2) become connected, or when the electrons from the upper sublevel (-1/2) and the excitons from the lower dark sublevel (+1/2, +3/2) become connected (dotted lines in Fig. 5). In the first case in sufficiently high magnetic fields and at low temperatures the exciton concentration on the upper sublevel is small and in the second case the electron concentration on the upper sublevel is small. Hence, in both cases the concentration of the singlet trion is small.

Similarly, the lower Zeeman sublevel of the singlet trion becomes populated when the electrons from the lower sublevel (s = +1/2) and the dark excitons from the upper sublevel (-1/2, -3/2) become connected, or when the electrons from the upper (-1/2) and the bright excitons from the lower sublevel (+1/2, -3/2) become connected (solid lines in Fig. **??**).

In the first case the concentration of excitons on the upper sublevel is small. In the second case the concentration of the electrons on the upper sublevel is small. Thus, the concentration of the singlet trions on the low Zeeman sublevel is small too.

In contrast to the singlet trion, the triplet trion can be formed from the excitons and

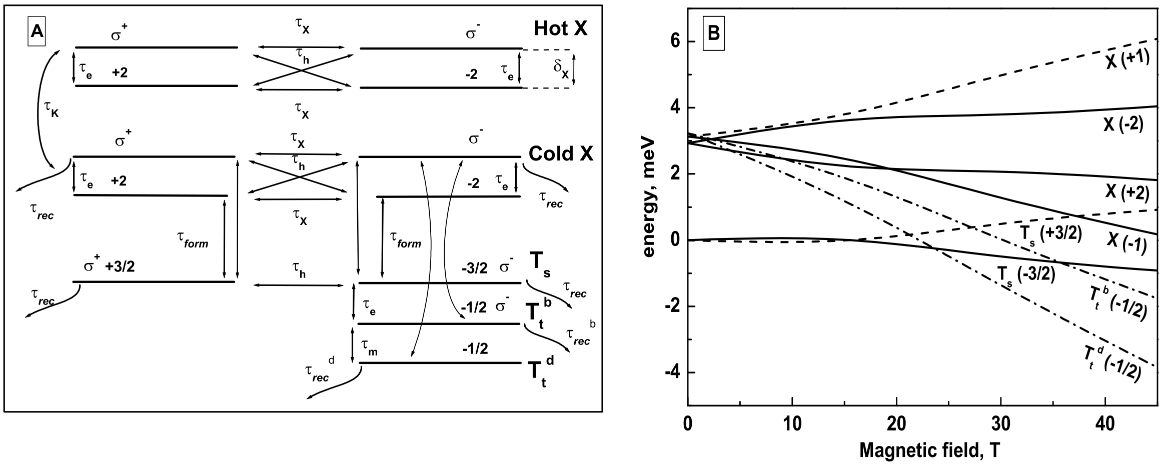


Figure 6: A) - Schematic representation of exciton and trion energy levels at H=0T; Hot X stands for hot excitons; Cold X - for cold excitons; $T_s$ - for singlet trion states; $T_t$ - for triplet trion states (bright and dark). B) - Energy levels of exciton and trion as a function of magnetic field.

electrons both depositing on low Zeeman sublevels. The triplet state with the projection of the full spin on $z$ axis $S_z^{trip}$ = -1/2: (+1/2, +1/2, -3/2) to which we ascribe the $T_t^d$ line, is formed by the electrons from the lowest Zeeman sublevel (+1/2) and the excitons from the lowest Zeeman sublevel (+1/2, -3/2). As the magnetic field increases, the state becomes predominantly populated as compared to other trion states.

Thus, the intensity of the singlet trion PL line should fall in both polarizations, while the intensity of the $T_t^d$ line rises in $\sigma^-$, as the magnetic field grows. Due to the same reason the intensity of the neutral exciton line X rises with the growth of the magnetic field in $\sigma^-$ polarization.

Despite the fact that the optical transition from the lowest triplet trion state is forbidden by orbital momentum [RPV01, DS00, WQH00] this line can be observed owing to the preferable population in magnetic fields.

## 3.4 Calculation of the exciton-trion energetic system

A model calculation of the multilevel exciton-trion system using 12 kinetic equations was carried out. Thus, we consider four levels of hot excitons, for levels of cold excitons ($\pm$ 2, $\pm$1), two levels of singlet trion states ($\pm$3/2), two levels of triplet trion states - dark and bright (-1/2) and the electron levels. The equations used can be represented in form:

$$\frac{\partial n_i}{\partial t} = \Sigma(n_j w_{ji} - n_i w_{ji}) + g_i - n_i/\tau_i^{rec}. \tag{4}$$

Here $n_i$ is the exciton concentration on the $i$-th level, $w_{ij}$ is the transition rate from the $i$-th level to the $j$-th level, $g_i$ and $n_i/\tau_i^{rec}$ are the generation and recombination rates for the $i$-th level, correspondingly. The transition rate between levels $i$ and $j$ is proportional to the inverse relaxation time from the $i$-th to $j$-th level $1/\tau_{ij}$ The transition rates within the sublevels of the same kind (hot excitons; cold excitons; trions) are simply related by the thermal equilibrium condition described by the Boltzman distribution $w_{ij}/w_{ji} = exp(\Delta_{ij}/KT)$ , where $\Delta_{ij}= E_i - E_j$ is the energy difference between i-th and j-th levels.

The electron levels are populated according to the Fermi distribution among all electron Landau levels.

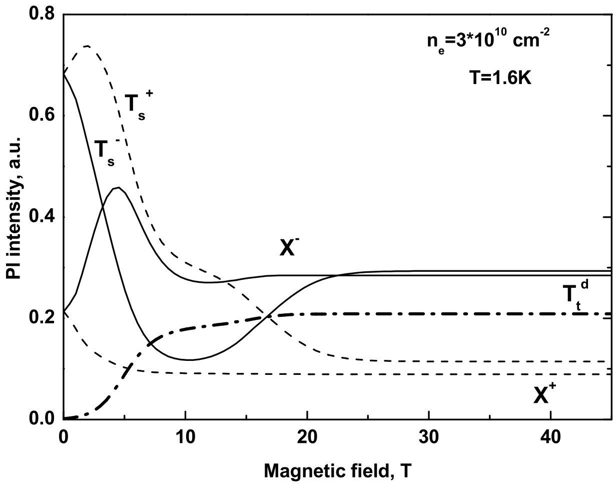


Figure 7: Calculated magnetic field dependencies of the intensities of all the PL lines: Exciton - X, Singlet trion - $T_s$ in $\sigma^+$ (dashed lines) and $\sigma^-$ (solid lines) circular polarizations and dark triplet $T_t^d$ - dot-dashed curves.

he relaxation and radiative recombination processes were taken into account with characteristic time for each of the processes. We assumed that the exciton spin could relax independently in addition to the relaxation by consecutive spin flips of electron and hole. The values for the characteristic times were chosen as follows: the trion formation time (for triplet and singlet states) $\tau_{form} = 10$ ps, the electron spin relaxation time $\tau_e = 150$ ps and the hole spin relaxation time $\tau_h = 70$ ps, the spin relaxation time of exciton as a whole $\tau_X = 30$ ps, the relaxation time between bright triplet and dark triplet $\tau_m = 40$ ps, the hot exciton thermalization time $\tau_k = 12$ ps, the exciton and singlet trion radiative lifetime $\tau_{rec}^X = 40$ ps and $\tau_{rec}^{T_s} = 60$ ps respectively, the dark triplet trion radiative lifetime $\tau_{rec}^{T_t^d} =$ (50-100)*$\tau_{rec}^{T_s}$ and the bright triplet radiative lifetime $\tau_{rec}^{T_t^b} = 80$ ps. The splitting between optically dark excitons with $S_z = \pm 2$ and optically active excitons with $S_z = \pm 1$ was taken to be $\delta_X = 0.2$ meV. [JCM+02]

Fig. 7 shows the calculated dependencies of the luminescence intensity of all the spectral lines on the magnetic fields. There is a good agreement between the experimental (Fig. 4) and calculated dependencies.

Fig. 7 shows that though the probability of the optical transition from the dark triplet trion state was chosen to be two orders of magnitude less than that of the allowed transition, the dark triplet trion PL line should be clearly seen in the PL spectra in the magnetic field as low as 7 T. As the magnetic field grows its intensity rises and saturates in the field about 23 T. The intensity of the dark triplet trion PL line is comparable with that of the exciton luminescence line.

This behavior of the triplet trion line is due to the preferable formation of exactly this triplet trion state in the magnetic field. Because the PL intensity is proportional to the product of the inverse radiative lifetime and the level population, the PL of the dark trion can be rather strong even in the case of large radiative lifetime as we have for the dark triplet.

# 4 CONCLUSIONS

Photoluminescence and reflectivity spectra have been taken from $Cd_{0.7}Mg_{0.3}Te/CdTe$ modulation doped quantum well in high magnetic fields. The following results were obtained:

1. Optically allowed and optically forbidden triplet trion states have been observed.

2. Binding energies of the triplet trion states have been measured as a function of magnetic fields.

3. A model that explained the appearance of the dark triplet in the PL spectra has been developed. The model allows to conclude that the formation of optically active singlet trion state is suppressed by magnetic fields whereas the formation of optically inactive triplet trion state is facilitated by magnetic fields.

4. The model calculation of the exciton – trion system has been made to describe the observed magnetic field dependencies of PL intensities.

# References


[AKY+02] G. V. Astakhov, V. P. Kochereshko, D. R. Yakovlev, W. Ossau, J. Nuernberger, W. Faschinger, G. Landwehr, T. Wojtowicz, G. Karczewski, and J. Kossut. *Phys. Rev. B*, 65:115310, 2002.

[BS57] H. A. Bethe and E. E. Salpiter. Quantum mechanics of one and two-electron atoms, 1957.

[DS00] A. B. Dzyubenko and A. Yu. Sivachenko. *Phys. Rev. Lett*, 56:4429, 2000.

[JCM+02] C. R. L. P. N. Jeukens, P. C. M. Christianen, J. C. Maan, D. R. Yakovlev, W. Ossau, V. P. Kochereshko, T. Wojtowicz, G. Karczewski, and J. Kossut. *Phys. Rev. B*, 66:235318, 2002.

[KCM+93] K. Kheng, R. T. Cox, D. Y. Merle, F. Bassani, K. Saminadayar, and S. Tatarenko. *Phys. Rev. Lett.*, 71:1752, 1993.

[RPV01] C. Riva, F. M. Peeters, and K. Varga. *Phys. Rev. B*, 63:115302, 2001.

[WKK+97] T. Wojtowicz, M. Kutrowski, G. Karczewski, G. Cywinski, M. Surma, J. Kossut, D. R. Yakovlev, W. Ossau, G. Landwehr, and V. Kochereshko. *Acta. Phys. Pol. A*, 92:1063, 1997.

[WQH00] A. Wojs, J. J. Quinn, and P. Hawralak. *Phys. Rev. B*, 62:4630, 2000.